THE NEW AXIAL BUNCHER AT INFN-LNS

A. Caruso, G. Gallo, A. Longhitano INFN-LNS, Catania, Italy
J. Sura, Warsaw University, Warsaw, Poland
F. Consoli, Associazione Euratom-ENEA sulla Fusione, Frascati, Italy
Li Pengzhan, China Institute of Atomic Energy, Beijing, China

Abstract

A new axial buncher for the K-800 superconducting cyclotron is under construction at LNS [1]. This new device will replace the present buncher [2] installed along the vertical beam line, inside the yoke of the cyclotron at about half a meter from the medium plane. Maintenance and technical inspection are very difficult to carry out in this situation. The new buncher will still be placed along the axial beam line, just before the bottom side of the cyclotron yoke. It consists of a drift tube driven by a sinusoidal RF signal in the range of 15-50 MHz, a matching box, an amplifier, and an electronic control system. A more accurate mechanical design of the beam line portion will allow for the direct electric connection of the matching box to the ceramic feed-through and drift tube. This particular design will minimize, or totally avoid, any connection through coaxial transmission line. It will reduce the entire geometry, the total RF power and the maintenance. In brief, the new axial buncher will be a compact system including beam line portion, drift tube, ceramic feed-through, matching box, amplifier and control system interface in a single structure.

BUNCHER STUDY

This new device will be driven by a simple sinusoidal voltage, as the rough approximation of the ideal saw-tooth signal [3]. The sine wave choice will reduce the total efficiency and performance of the system, but the generation of a high frequency saw-tooth in the range 15-50 MHz remains difficult still today. The basic two-gap buncher structure [4] is shown in Fig.1, between the SERSE ion source [5] and the K-800 superconducting cyclotron.

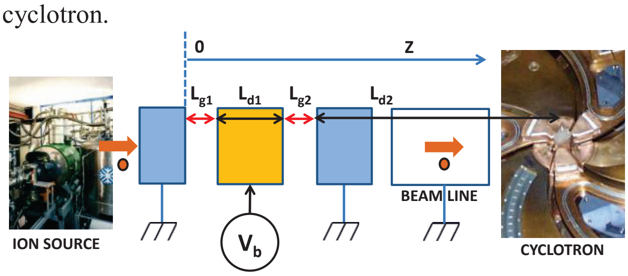

Figure 1: Basic structure of the axial buncher.

It is a drift tube, fed by the sinusoidal voltage $V_B = V_{MB}\sin(\omega t + \varphi_0)$, and placed between two grounded tube electrodes. L_{g1} and L_{g2} are the two gaps of 5 mm length. The distance between the Buncher and the inflector at the cyclotron central region is 3011 mm, and it is imposed by mechanical constraints. Particles generated by the ion source have $v_{z0} = \sqrt{2q_i V_s/m_i}$ velocity, being q_i and m_i their charge and mass, and V_s the voltage of the source output electrode. The drift tube length L_{d1} is 83.5 mm. This length is chosen so that L_{d1}+L_{g1} is an odd integer multiple of the $\beta\lambda/2$ quantity. In particular, $\beta\lambda = v_{z0}/f$ (with f cyclotron frequency) is the path of the particles in one period and, because of the fixed geometry of the cyclotron central region, has to be constant.

The basic theoretical study of the bunching effect in the present structure [4] has been analytically performed here by considering a time-varying and spatially uniform electric field within the two L_{g1} and L_{g2} gaps. Here particles undergo a time varying acceleration, whereas they will move in uniform linear motion within the following drift tubes. We now illustrate the typical case for α particles. It gives: $V_{MB} = 73.8078$ V, $V_S =$ 24.72 kV, f = 43.617 MHz, and then $\beta\lambda = 35.28$ mm. The cyclotron acceptance interval phase is 35°. Each particle of the continuous flow coming from the ion source arrives at the position z = 0 at the t_0 time instant (Fig. 1). The calculated particle trajectories are shown in Fig. 2a-2b in the Applegate diagrams, referred to one period. The trajectories grouping is apparent. The time instants when they reach the cyclotron inflector is t_{d2}. In Fig. 2c-2d the plot of t_{d2} versus t_0/T is shown. The V_{MB} voltage has been tailored to optimize the particle transmission within the cyclotron acceptance time, referred to the 35° phase. This is clearly shown in Fig. 2c-2d, where the curve is tangent to the dotted boundaries.

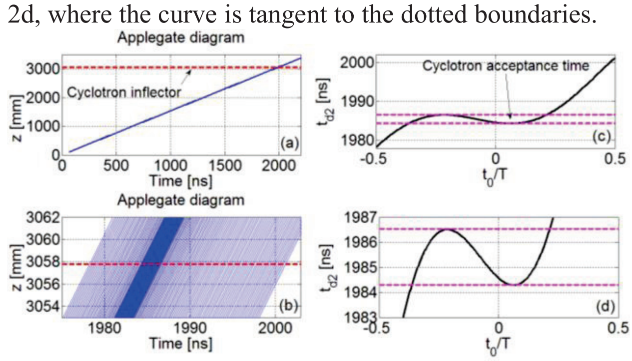

Figure 2: (a) and (b) Applegate diagrams with different scales; (c) and (d) t_{d2} versus t_0/T.

Under these conditions the particle transmission to the cyclotron is TR = 57.6%, and the energy spread is $\Delta E/E$ = 1.15%.

ISBN 978-3-95450-128-1

BUNCHER DESIGN

The main components of the axial buncher can be divided in two blocks: mechanic and electrical.

Mechanical Design

The mechanics (see Fig. 3) include the drift tube (c) and the ground electrodes (b) inside a four-gate beam line section (a). A standard vacuum ceramic feed-through connects the drift tube with the external RF signal. Fig. 3d shows the position of the buncher along the axial beam line - the human body on the reference plane gives a rough scale factor of the full size dimension. The distance between the centre of the drift tube and time focus is about 3m.

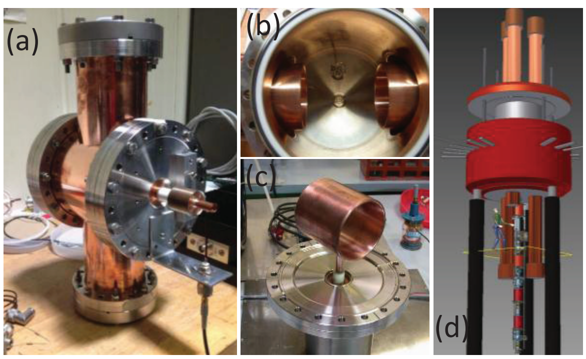

Figure 3: Buncher mechanic (a,b,c) and cyclotron (d).

The beam line section dimensions are 403 and 176 mm, in length and width respectively. The upper and lower flanges, in/out beam, are DN100CF. The horizontal central orthogonal flanges are two standard DN160CF. The Fig. 3c shows the ceramic feed-through connected to the drift tube assembled on one of the two DN160CF. The other DN160CF hosts a pair of RF pick-ups, see Fig. 3b. The drift tube is copper made, while a galvanic deposition of copper of a few hundred µm (well above the skin effect) has been placed on the ground electrodes and the standard steel cross section beam line. In this way all the surfaces are in copper, except the flanges relative to the feed-through and pick-up. The copper deposition has increased the total Q factor of the system which prevents and/or minimizes any copper surface facing a steel surface under high vacuum. The length, the inner diameter and the thickness of the drift tube are 83.5, 75 and 2.5 mm respectively.

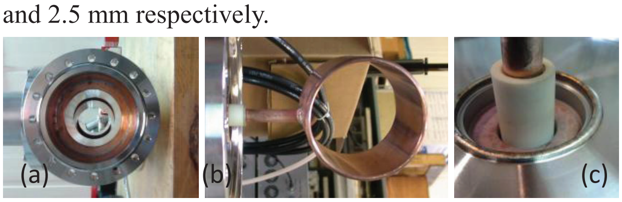

Figure 4: TIG welding technique.

A soft soldering has been adopted to connect the feed-through to the drift tube (copper-copper) and a T.I.G. welding has been adopted to weld the flange at ground (steel-steel), see Fig. 3b-c. The same welding technique to connect the ground electrodes to the beam line has been adopted, see Fig. 4a.

Electrical Design

From the electrical point of view the drift tube can be seen as a capacitance. The specific N-type coaxial adaptor (see Fig. 5b) allows the connection between the feed-through and the measuring instruments. An LCR meter confirms the simulated capacitance value of about 27pF and, with a vector network analyser, the self-resonance of 352,75 MHz has been measured, too (see Fig. 5a).

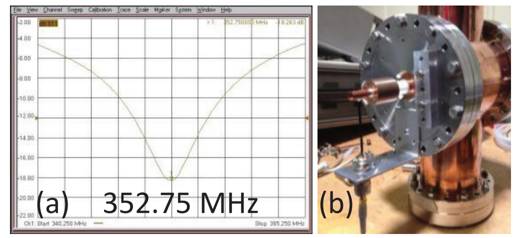

Figure 5: (a) Self-resonance, (b) N-type adaptor.

The frequency range of the axial buncher is identical to the cyclotron's, between 15 and 50 MHz. A matching circuit has been developed to adapt the input of the buncher to the standard impedance of 50 Ω for all the frequency bandwidths. The matching box schematic between the drift tube and the 50Ω is shown in Fig. 6.

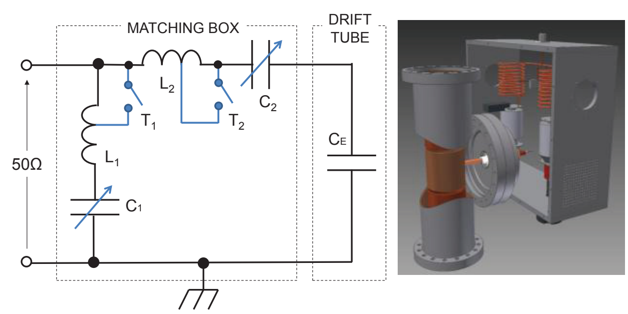

Figure 6: Matching-tuning box and drift tube.

The schematic of Fig. 6 is an impedance transformer, from $Z_0=50\Omega$ to Z_b, where Z_b is the impedance seen at the input of the feedthrough. The input impedance of the transformer can be calculated (see Eq.1).

$$Z_{in} = \frac{Z_{shunt} \cdot (Z_{series} + Z_b)}{Z_{shunt} + (Z_{series} + Z_b)}. \quad (1)$$

Where Z_{ser} and Z_{sh} are the series and shunt impedance of the L_2C_2 and L_1C_1 circuits. If we assume $Z_{in}=Z_0$ the matching is done for the whole bandwidth.C1 and C_2 are two vacuum multi-turn variable capacitors from 5 to 500 pF and L_1 and L_2 are two 'selectable' inductors. The range 15-50 MHz, too large for two fixed inductors, has been divided in two bandwidths, the lower ($L_1=L_2=4.2\mu H$) and the upper ($L_1=L_2=1.3\mu H$). The bandwidth is selectable, from low to high, by the commutation of a double relay contact, T_1 and T_2. If T_1 and T_2 are open, the minimum working frequency is less than 15 MHz, whereas if T_1 and

T_2 are closed, the maximum frequency is above 50 MHz, the full range is covered. A specific design of the beam line portion will allow for the direct electrical connection of the matching box to the drift tube, see Fig. 7. This particular design prevents any connection through coaxial transmission line. It reduces the entire geometry, the connection losses, the total RF power and the maintenance.

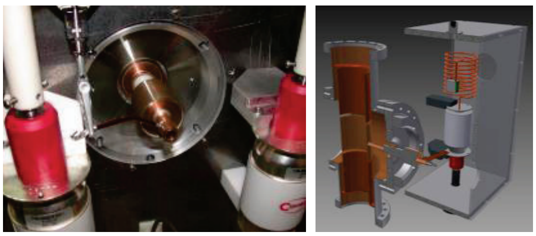

Figure 7: Direct connection between drift-tube and matching box.

Some numerical simulations have been developed to calculate, for all the operative frequencies, the capacitance values of C_1 and C_2, the buncher voltage, V_{MB}, at the drift tube and the relative RF power applied at the matching box. V_{MB} will be between 64 and 110 V, for an RF power of 1-2 W, only. Assuming V_B=80 V, the simulated potential (a) and electrical field distribution (b) are symmetrically in y-z plane, as shown in Fig. 8.

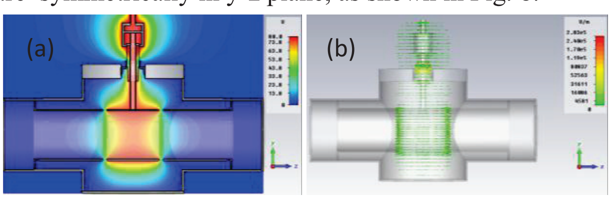

Figure 8: Potential (a). 3D electric field distribution (b).

ELECTRONIC CONTROL SYSTEM

The electronic control system is based on the general Low Level RF-Box, developed in-house [6]. It includes in one single rack the functions of protections, turn-on and RF-generator (DDS-based). The matching box control panel sets and checks the two variable capacitors, selects the inductors according to the lower-upper bandwidth, switches on-off and/or bypasses the power amplifier in case of tuning operation. Figure 9 shows the control panels.

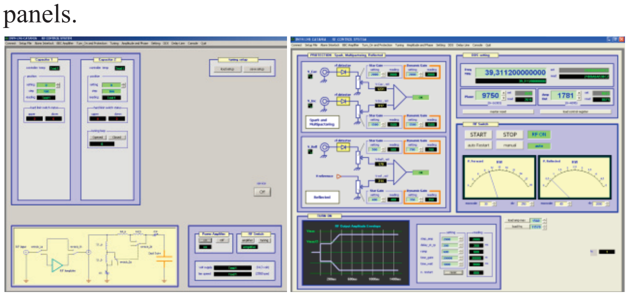

Figure 9: Axial buncher control panels.

TEST AND MEASUREMENTS

The main components and the block diagram of the test bench are: RF synthesizer, power amplifier, directional coupler, matching-box and drift tube inside the beam line section under vacuum (2.8x10^{-6}mbar). See Fig. 9.

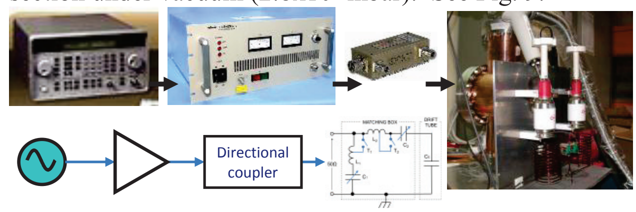

Figure 9: Test bench of the axial buncher at LNS.

The whole frequency bandwidth has been accomplished in terms of impedance matching and drift tube voltages. The minimum and maximum frequencies cover more than the bandwidth itself with a VSWR≅1 (see Fig. 10).

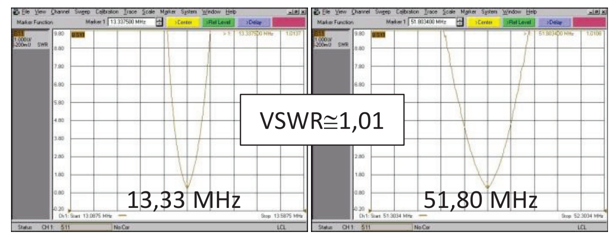

Figure 10: Min. and max. measured frequencies.

Further S-parameter measurements and drift tube voltage measurements are shown in Fig. 11.

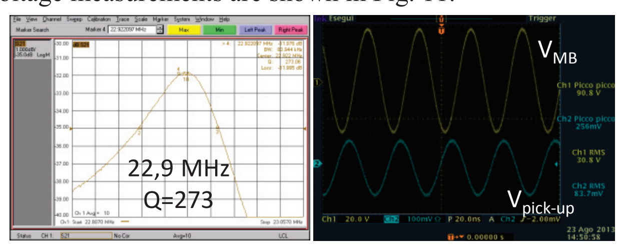

Figure 11: Q-factor , drift tube and pick-up voltages.

CONCLUSION

All RF tests and measurement have been achieved at full power on the test bench. The cyclotron long maintenance programme has delayed the final test on the axial beam line of the new buncher. We believe we can produce a first test on the beam at the beginning of 2014.

ACKNOWLEDGMENT

A special thanks goes to B. Trovato and his workshop staff for their skillful assistance in the mechanics.

REFERENCES

[1] D. Rifuggiato et al., "Variety of beam production at the INFN LNS Superconducting Cyclotron", M0PPT011, these proceedings.
[2] L. Calabretta et al., The Radiofrequency Pulsing System at INFN-LNS, USA, CYCLOTRONS 2001, p. 297.
[3] C. Goldstein and A. Laisne, NIM 61, 221, 1968.
[4] W.J.G.M. Kleeven et al., NIM B 64, 367, 1992.
[5] S. Gammino et al., Review of scientific instruments volume 70, nr. 9 September 1999.
[6] A. Caruso et al., MOPCP057 Proceedings of CYCLOTRONS 2010, Lanzhou, China, p. 159.

ISBN 978-3-95450-128-1